


## Article

# Rational Design, Synthesis, Separation, and Characterization of New Spiroindoles Combined with Benzimidazole Scaffold as an MDM2 Inhibitor

Saeed Alshahrani <sup>1</sup>, Abdullah Mohammed Al-Majid <sup>1</sup>, M. Ali <sup>1</sup>, Abdullah Saleh Alamary <sup>1</sup>,  
Marwa M. Abu-Serie <sup>2</sup>, Alexander Dömling <sup>3</sup>, Muhammad Shafiq <sup>4</sup>, Zaheer Ul-Haq <sup>4</sup> and Assem Barakat <sup>1,\*</sup>

<sup>1</sup> Department of Chemistry, College of Science, King Saud University, P.O. Box 2455, Riyadh 11451, Saudi Arabia

<sup>2</sup> Medical Biotechnology Department, Genetic Engineering and Biotechnology Research Institute, City of Scientific Research and Technological Applications (SRTA-City), Alexandria 21934, Egypt

<sup>3</sup> Department of Drug Design, Groningen Research Institute of Pharmacy, University of Groningen, 9713 AV Groningen, The Netherlands

<sup>4</sup> Dr. Panjwani Center for Molecular Medicine and Drug Research, International Center for Chemical and Biological Sciences, University of Karachi, Karachi 75270, Pakistan

\* Correspondence: ambarakat@ksu.edu.sa

**Abstract:** Rational design for a new spiroindoles, combined with a benzimidazole scaffold to identify a new murine double minute two (MDM2) inhibitor was synthesized and characterized. The desired spiroindoles were achieved *via* a [3+2] cycloaddition reaction approach which afforded the cycloadducts with four asymmetric centers separated in an excellent regioselective and diastereoselective compound. The separated spiroindoles were subjected to a set of biochemical assays including an NCI cell panel assay, MTT assay, and MDM2 binding analysis by a microscale thermophoresis assay. The anticancer reactivity for the tested compounds showed IC<sub>50</sub> (μM) in the range between 3.797–6.879 μM, and compound **7d** with IC<sub>50</sub> = 3.797 ± 0.205 μM was the most active candidate between the series. The results showed promising results that identified that compound **7a** could be inhibited the MDM2 with K<sub>D</sub> = 2.38 μM. Compound **7a** developed a network of interactions with the MDM2 receptor studied *in silico* by molecular docking.

**Keywords:** spiroindole; benzimidazole; MDM2



**Citation:** Alshahrani, S.; Al-Majid, A.M.; Ali, M.; Alamary, A.S.; Abu-Serie, M.M.; Dömling, A.; Shafiq, M.; Ul-Haq, Z.; Barakat, A. Rational Design, Synthesis, Separation, and Characterization of New Spiroindoles Combined with Benzimidazole Scaffold as an MDM2 Inhibitor. *Separations* **2023**, *10*, 225. <https://doi.org/10.3390/separations10040225>

Academic Editors: Yasser A. El-Amier and Ahmed A. Al-karmalawy

Received: 13 February 2023  
Revised: 9 March 2023  
Accepted: 16 March 2023  
Published: 24 March 2023



**Copyright:** © 2023 by the authors. Licensee MDPI, Basel, Switzerland. This article is an open access article distributed under the terms and conditions of the Creative Commons Attribution (CC BY) license (<https://creativecommons.org/licenses/by/4.0/>).

## 1. Introduction

The MDM2–p53 protein–protein interaction inhibitor is a hot research topic and has been gaining a lot of attention recently [1–4]. The inhibition of the interaction between the two proteins, p53, and MDM2, leads to reactivation of the p53 which has many functionalities, including DNA repairing, apoptosis, cell cycle arrest, senescence, metabolic alteration, and tumor suppressor [5,6]. The mutant p53 protein has been found in approximately 50% of human cancer cells [7,8]. The dislocation between the MDM2 protein and p53 protein is a challenge and is important to the development of a new chemotherapeutic agent.

Based on the literature survey, it has been reported so far that more than 20 chemotypes of molecules have been identified as MDM2–p53 inhibitors such as spirooxindoles [9], nutlins [10], isoquinoline-1-one [11], chalcone [12], pyrrolin-2-one [13], piperidine [14], morpholinone [15], imidazolyl indole [16], benzodiazpinedione [17], diketopiperazines [18], chromenotriazolopyrimidines [19], and other pharmacophores. For this, protein–protein interaction (PPI) inhibitors have progressed into clinical trials including spirooxindoles such as APG-115 [20], SAR405838 [21], and other pharmacophores such as RG7388 [22], HDM201 [23], RG7112 [24], and AMG-232 [25]. Inhibiting the p53–MDM2 interaction is a promising strategy for cancer treatment, as it can help to restore normal cell growth and death.

Protein–protein interaction inhibitors (PPIs) are typically small molecules that are designed to bind to the p53 and MDM2 proteins and prevent them from interacting. Several PPIs have been developed and are currently in clinical trials for a variety of cancers. Common side effects including fatigue, nausea, and anemia were observed.

In between the small molecules reported as promising lead compounds for cancer research are the spirooxindoles. This scaffold is able to activate the p53 and bind with the MDM2 domain [26–47]. Spirotryprostatin B is an inspired natural product that exhibits anticancer reactivity [33] (Figure 1). Gollner A. et al. reported a novel chemically stable spiro [3*H*-indole-3, 2'-pyrrolidin]-2 (1*H*)-one lead compound and orally active inhibitors of the MDM2–p53 interaction [34]. Benzimidazole scaffold was introduced to many compounds which showed high efficacy against MDM2, MDMX, and NF-κB inhibitors [40–46]. Our research group has engaged in this research program for a couple of years and has been successful in designing and developing several molecules towards PPI [35–39]. Among the discovered molecules, a new spirooxindole [48], as a rigid structure with a combination of benzimidazole scaffold, has been discovered as a novel MDM2 protein inhibitor with dual effects of antimetastatic efficacy. Based on these findings, we have rationally designed and synthesized a new spirooxindoles-based benzimidazole unit as an MDM2 inhibitor.

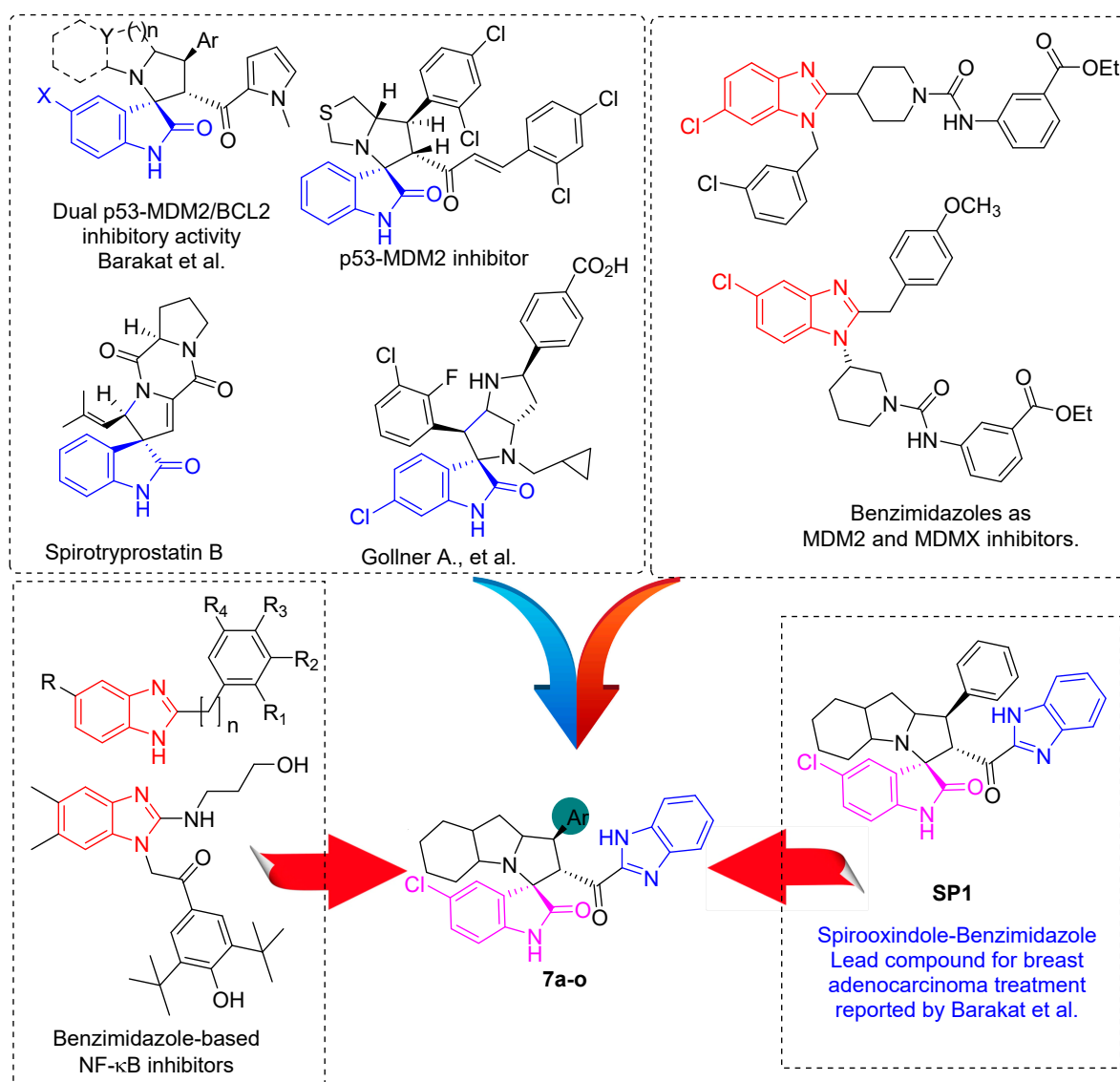


**Figure 1.** Reported spirooxindoles and benzimidazoles with anticancer activity and our rationally designed compound 7a-o [34,36].

## 2. Materials and Methods

### 2.1. General

“All chemicals were purchased from Aldrich, Sigma-Aldrich and Fluka, which were used without further purification unless otherwise stated. All melting points were measured using a Gallenkamp melting point apparatus in open glass capillaries and were uncorrected. Crude products were purified by column chromatography on silica gel of 100–200 mesh. IR spectra were measured as KBr pellets using a Nicolet 6700 FT-IR spectrophotometer. The NMR spectra were recorded using a Varian Mercury Jeol-400 NMR spectrometer.  $^1\text{H}$  NMR (400 MHz) and  $^{13}\text{C}$  NMR (100 MHz) spectroscopy were performed in either deuterated dimethylsulfoxide (DMSO- $d_6$ ) or deuterated chloroform ( $\text{CDCl}_3$ ). Chemical shifts ( $\delta$ ) are reported in terms of ppm and coupling constants  $J$  are given in Hz. Elemental analysis was carried out using an Elmer 2400 Elemental Analyzer in CHN mode”.

### 2.2. Synthesis of Spirooxindole Analogues (7a-o) General Procedure

Chalcone derivative **4a-o** (0.5 mmol), octahydroindole-2-carboxylic acid **6** (84.62 mg, 0.5 mmol), and 5-chlorisatin **5** (90.79 mg, 0.5 mmol) were mixed in 20 mL MeOH then, heated up at 60–65 °C for 2–3 h. After the reaction was completed, as monitored by TLC, the crude material was subjected to column chromatography using ethylacetate/n-hexane (2: 6), yielding spiro compounds in pure form.

#### **2'-(1H-Benzo[d]imidazole-2-carbonyl)-5-chloro-1'-(4-chlorophenyl)-1',2',4a',5',6',7',8',8a',9',9a'-decahydrospiro[indoline-3,3'-pyrrolo[1,2-a]indol]-2-one (7a).**

Pale yellow solid; yield (80%); m.p.:176–178 °C; IR (KBr,  $\text{cm}^{-1}$ ): 3434 (NH), 3277 (NH), 3093 (CH), 2929 (CH),1729 (CO), 1682 (CO);  $^1\text{H}$ -NMR (DMSO- $d_6$ , 400 MHz):  $\delta$  12.98 (1H, s, NH), 10.17 (1H, s, NH), 7.73 (1H, s, Ph-H) 7.45 (2H, d,  $J = 8.0$  Hz, Ph-H), 7.42–7.26 (6H, m, Ph-H), 7.08 (1H, d,  $J = 8.0$  Hz, Ph-H), 6.44 (1H, d,  $J = 8.0$  Hz, Ph-H), 5.29 (1H, d,  $J = 11.9$  Hz,  $\text{CHCO}$ ), 4.00 (2H, m,  $\text{CHN}$ ,  $\text{CHPh}$ ), 3.23 (1H, d,  $J = 3.7$  Hz), 2.16–2.08 (1H, m), 2.06–1.98 (1H, m), 1.55–0.70 (10H, m, aliphatic CH); Anal. for  $\text{C}_{32}\text{H}_{28}\text{Cl}_2\text{N}_4\text{O}_2$ ; calcd: C, 67.25; H, 4.94; N, 9.80 Exper.: C, 66.89; H, 5.03; N, 10.04.

#### **2'-(1H-Benzo[d]imidazole-2-carbonyl)-5-chloro-1'-(4-(trifluoromethyl)phenyl)-1',2',4a',5',6',7',8',8a',9',9a'-decahydrospiro[indoline-3,3'-pyrrolo[1,2-a]indol]-2-one (7b).**

Pale yellow solid; yield (32%); m.p.:125–127 °C; IR (KBr,  $\text{cm}^{-1}$ ): 3429 (NH), 3282 (NH), 3099 (CH), 2927 (CH),1724 (CO), 1686 (CO);  $^1\text{H}$ -NMR (DMSO- $d_6$ , 400 MHz):  $\delta$  12.98 (1H, s, NH), 10.20 (1H, s, NH), 7.75 (1H, d,  $J = 8$  Hz, Ph-H), 7.68 (4H, m, Ph-H), 7.48–7.20 (4H, m, Ph-H), 7.09 (1H, d,  $J = 8.8$  Hz, Ph-H), 6.43 (1H, d,  $J = 8.3$  Hz, Ph-H), 5.34 (1H, d,  $J = 11.7$  Hz,  $\text{CHCO}$ ), 4.11 (1H, m,  $\text{CHN}$ ), 3.46 (1H, m,  $\text{CHPh}$ ), 2.10 (2 H, d,  $J = 12.9$ Hz), 1.58–0.67 (10 H, m, aliphatic C-H); Anal. for  $\text{C}_{33}\text{H}_{28}\text{ClF}_3\text{N}_4\text{O}_2$ ; calcd: C, 65.51; H, 4.66; N, 9.26 Exper.: C, 66.09; H, 4.77; N, 9.14.

#### **2'-(1H-Benzo[d]imidazole-2-carbonyl)-5-chloro-1'-(p-tolyl)-1',2',4a',5',6',7',8',8a',9',9a'-decahydrospiro[indoline-3,3'-pyrrolo[1,2-a]indol]-2-one (7c).**

Yellow solid; yield (41%); m.p.:163–165 °C; IR (KBr,  $\text{cm}^{-1}$ ): 3649 (NH), 3277 (NH), 3087(CH), 2926 (CH),1727 (CO), 1690 (CO);  $^1\text{H}$ -NMR (DMSO- $d_6$ , 400 MHz):  $\delta$  12.98 (1H, s, NH), 10.18 (1H, s, NH), 7.76 (1H, d,  $J = 8.0$  Hz, Ph-H), 7.40 (1H, d,  $J = 2.2$  Hz, Ph-H), 7.35–7.26 (5H, m, Ph-H), 7.10–7.06 (3H, d,  $J = 8.0$  Hz, Ph-H), 6.44 (1H, d,  $J = 8$  Hz, Ph-H), 5.34 (1H, d,  $J = 12.4$  Hz,  $\text{CHCO}$ ), 4.11–4.00 (1H, m,  $\text{CHN}$ ), 3.96–3.86 (1H, m,  $\text{CHPh}$ ), 2.20 (3H, s,  $\text{CH}_3$ ), 2.11 (2 H, d,  $J = 8.0$ Hz), 1.56–0.72 (10H, m, aliphatic C-H);  $^{13}\text{C}$ -NMR (DMSO- $d_6$ , 100 MHz):  $\delta = 189.91, 180.05, 148.02, 143.07, 141.62, 136.60, 136.47, 135.18, 129.69, 127.85, 126.33, 125.17, 123.63, 111.02, 71.74, 63.94, 57.24, 52.79, 36.80, 28.19, 25.07$ ; Anal. for  $\text{C}_{33}\text{H}_{31}\text{ClN}_4\text{O}_2$ ; calcd: C, 71.92; H, 5.67; N, 10.17 Exper.: C, 71.59; H, 5.71; N, 10.44.

#### **2'-(1H-Benzo[d]imidazole-2-carbonyl)-5-chloro-1'-(thiophen-2-yl)-1',2',4a',5',6',7',8',8a',9',9a'-decahydrospiro[indoline-3,3'-pyrrolo[1,2-a]indol]-2-one (7d).**

Pale yellow solid; yield (48%); m.p.:130–132 °C; IR (KBr,  $\text{cm}^{-1}$ ): 3624 (NH), 3258 (NH), 3091(CH), 2927 (CH),1728 (CO), 1689 (CO);  $^1\text{H-NMR}$  ( $\text{CDCl}_3$ , 400 MHz):  $\delta$  10.18 (1H, s, NH), 8.64 (1H, s, NH), 7.84 (1H, d,  $J = 8.0$  Hz, Ph-H), 7.34 (1H, d,  $J = 8.0$  Hz, thio-H), 7.31–7.20 (4H, m, Ph-H), 6.99 (1H, d,  $J = 3.5$  Hz, thio-H), 6.95 (1H, dd,  $J = 8.2, 1.7$  Hz, thio-H), 6.90–6.85 (1H, m, Ph-H), 6.39 (1H, d,  $J = 8.6$  Hz, Ph-H), 5.30 (1H, d,  $J = 12.0$  Hz,  $\text{CHCO}$ ), 4.53–4.34(1H, m,  $\text{CHN}$ ), 4.12 (1H, t,  $J = 11.0$  Hz,  $\text{CHPh}$ ), 3.20 (1H, d,  $J = 4.0$  Hz), 2.16 (1H, d,  $J = 5.0$ Hz), 1.83–0.82 (10 H, m, aliphatic C-H);  $^{13}\text{C-NMR}$  ( $\text{CDCl}_3$ , 100 MHz):  $\delta = 189.65, 181.65, 146.83, 143.16, 141.99, 139.94, 133.80, 129.28, 126.77, 125.88, 123.80, 111.02, 72.12, 71.33, 65.76, 57.93, 48.77, 37.52, 28.38, 27.86, 19.70$ ; Anal. for  $\text{C}_{30}\text{H}_{27}\text{ClN}_4\text{O}_2\text{S}$ ; calcd: C, 66.35; H, 5.01; N, 10.32 Exper.: C, 66.49; H, 5.20; N, 10.14.

**2'-(1H-Benzo[d]imidazole-2-carbonyl)-5-chloro-1'-(4-fluorophenyl)-1',2',4a',5',6',7',8',8a',9',9a'-decahydrospiro[indoline-3,3'-pyrrolo[1,2-a]indol]-2-one (7e).**

Pale yellow solid; yield (35%); m.p.:148–150 °C; IR (KBr,  $\text{cm}^{-1}$ ): 3431 (NH), 3268 (NH), 3096 (CH), 2960 (CH),1732 (CO), 1684 (CO);  $^1\text{H-NMR}$  ( $\text{CDCl}_3$ , 400 MHz):  $\delta$  10.02 (1H, s, NH), 8.55 (1H, s, NH), 7.82 (1H, d,  $J = 8.3$  Hz, Ph-H), 7.40 (2 H, dd,  $J = 8.5, 5.4$  Hz), 7.35–7.12 (5H, m, Ph-H), 6.94 (3H, m, Ph-H), 6.36 (1H, d,  $J = 8$  Hz, Ph-H), 5.32 (1H, d,  $J = 12.4$  Hz,  $\text{CHCO}$ ), 4.31 (1H, q,  $J = 7.4$  Hz,  $\text{CHN}$ ), 3.79 (1H, t,  $J = 12.4$  Hz,  $\text{CHPh}$ ), 3.19–0.87 (12 H, m, aliphatic C-H);  $^{13}\text{C-NMR}$  ( $\text{CDCl}_3$ , 100 MHz):  $\delta = 189.71, 181.92, 163.19, 160.76, 146.85, 143.08, 139.91, 134.65, 134.62, 133.69, 129.56, 129.49, 129.30, 127.35, 126.82, 126.64, 126.09, 123.68, 122.61, 115.63, 115.42, 112.08, 110.91, 72.01, 71.26, 65.28, 57.78, 53.18, 41.88, 37.45, 29.79, 28.43, 27.82, 24.79, 19.75$ ; Anal. for  $\text{C}_{32}\text{H}_{28}\text{ClFN}_4\text{O}_2$ ; calcd: C, 69.25; H, 5.08; N, 10.09 Exper.: C, 69.49; H, 5.18; N, 10.44.

**2'-(1H-Benzo[d]imidazole-2-carbonyl)-5-chloro-1'-(2,4-dichlorophenyl)-1',2',4a',5',6',7',8',8a',9',9a'-decahydrospiro[indoline-3,3'-pyrrolo[1,2-a]indol]-2-one (7f).**

Pale yellow solid; yield (48%); m.p.:138–140 °C; IR (KBr,  $\text{cm}^{-1}$ ): 3436 (NH), 3281 (NH), 3090 (CH), 2925 (CH),1730 (CO), 1685 (CO);  $^1\text{H-NMR}$  ( $\text{CDCl}_3$ , 400 MHz):  $\delta$  10.14 (1H, s, NH), 8.40 (1H, s, NH), 7.84 (1H, d,  $J = 8.0$  Hz, Ph-H), 7.55 (1H, d,  $J = 8.7$  Hz, Ph-H), 7.37 (1H, s, Ph-H), 7.35–7.14 (5H, m, Ph-H), 6.95 (1H, d,  $J = 8.0$  Hz, Ph-H), 6.37 (1H, d,  $J = 8.0$  Hz, Ph-H), 5.39 (1H, d,  $J = 12.3$  Hz,  $\text{CHCO}$ ), 4.47 (1H, t,  $J = 11.0$  Hz,  $\text{CHPh}$ ), 4.20 (1H, q,  $J = 8.5$  Hz,  $\text{CHN}$ ), 3.20 (1 H, d,  $J = 4.4$  Hz), 2.14–0.89 (12 H, m, aliphatic C-H);  $^{13}\text{C-NMR}$  ( $\text{CDCl}_3$ , 100 MHz):  $\delta = 189.44, 181.66, 146.72, 143.03, 139.94, 135.42, 135.35, 133.76, 133.00, 129.56, 126.98, 125.98, 110.98, 71.87, 48.25, 27.66, 19.79$ ; Anal. for  $\text{C}_{32}\text{H}_{27}\text{Cl}_3\text{N}_4\text{O}_2$ ; calcd: C, 63.43; H, 4.49; N, 9.25 Exper.: C, 63.59; H, 5.04; N, 9.04.

**2'-(1H-Benzo[d]imidazole-2-carbonyl)-5-chloro-1'-(3-hydroxyphenyl)-1',2',4a',5',6',7',8',8a',9',9a'-decahydrospiro[indoline-3,3'-pyrrolo[1,2-a]indol]-2-one (7g).**

Pale yellow solid; yield (62%); m.p.:186–188 °C; IR (KBr,  $\text{cm}^{-1}$ ): 3626 (NH), 3257 (OH), 2931 (CH), 1726 (CO), 1688 (CO);  $^1\text{H-NMR}$  ( $\text{CDCl}_3$ , 400 MHz):  $\delta$  9.00 (1H, s, NH), 8.25 (1H, s, NH), 7.54 (1H, d,  $J = 4.0$  Hz, Ph-H), 7.46 (1H, s, OH), 7.22 (1H, d,  $J = 8.0$  Hz, Ph-H), 7.08–7.04 (3H, m, Ph-H), 6.89–6.72 (5H, m, Ph-H), 6.23 (1H, d,  $J = 8.0$  Hz, Ph-H), 5.31 (1H, d,  $J = 12.5$  Hz,  $\text{CHCO}$ ), 4.49–4.38 (1H, m,  $\text{CHN}$ ), 3.75–3.65 (1H, m,  $\text{CHPh}$ ), 3.14 (1H, d,  $J = 4$  Hz), 2.16–0.81 (12 H, m, aliphatic C-H); Anal. for  $\text{C}_{32}\text{H}_{29}\text{ClN}_4\text{O}_3$ ; calcd: C, 69.49; H, 5.29; N, 10.13 Exper.: C, 69.69; H, 5.14; N, 9.94.

**2'-(1H-Benzo[d]imidazole-2-carbonyl)-5-chloro-1'-(3,4,5-trimethoxyphenyl)-1',2',4a',5',6',7',8',8a',9',9a'-decahydrospiro[indoline-3,3'-pyrrolo[1,2-a]indol]-2-one (7h).**

Pale yellow solid; yield (88%); m.p.:160–162 °C; IR (KBr,  $\text{cm}^{-1}$ ): 3430 (NH), 3269 (NH), 3093 (CH), 2996 (CH),1722 (CO), 1683 (CO);  $^1\text{H-NMR}$  ( $\text{CDCl}_3$ , 400 MHz):  $\delta$  10.15 (1H, s, NH), 8.500 (1H, s, NH), 7.81 (1H, d,  $J = 8.0$  Hz, Ph-H), 7.37–7.19 (4H, m, Ph-H), 6.97 (1H, d,  $J = 8.4$  Hz, Ph-H), 6.66 (2H, s, Ph-H), 6.38 (1H, d,  $J = 8.5$  Hz, Ph-H), 5.38 (1H, d,  $J = 12.3$  Hz,  $\text{CHCO}$ ), 4.33 (1H, m,  $\text{CHPh}$ ), 3.78 (6H, s,  $\text{OCH}_3$ ), 3.73 (3H, s,  $\text{OCH}_3$ ), 3.19 (1H, m,  $\text{CHN}$ ), 2.02–0.78 (12 H, m, aliphatic C-H);  $^{13}\text{C-NMR}$  ( $\text{CDCl}_3$ , 100 MHz):  $\delta = 189.75, 181.68, 153.30, 146.99, 143.14, 139.85, 136.95, 134.53, 133.80, 133.31, 126.78, 126.18, 123.39, 122.48, 110.86,$

104.89, 72.25, 71.07, 60.86, 56.33, 56.18, 54.56, 41.84, 37.58, 28.44, 27.83, 24.76.; Anal. for C<sub>35</sub>H<sub>35</sub>ClN<sub>4</sub>O<sub>5</sub>; calcd: C, 67.03; H, 5.63; N, 8.93 Exper.: C, 67.59; H, 5.34; N, 9.05.

**2'-(1H-Benzo[d]imidazole-2-carbonyl)-5-chloro-1'-(2-hydroxyphenyl)-1',2',4a',5',6',7',8',8a',9',9a'-decahydrospiro[indoline-3,3'-pyrrolo[1,2-a]indol]-2-one (7i).**

Yellow solid; yield (82%); m.p.:128–130 °C; IR (KBr, cm<sup>-1</sup>): 3311 (OH), 3063 (CH), 2925 (CH),1716 (CO), 1667 (CO); <sup>1</sup>H-NMR (CDCl<sub>3</sub>, 400 MHz): δ 10.57 (1H, s, NH), 8.93 (1H, s, NH), 7.80 (1H, d, J = 8.0 Hz, Ph-H), 7.49 (1H, d, J = 8.0 Hz, Ph-H), 7.29 (2H, d, J = 7.3 Hz, Ph-H), 7.23 (1H, s, OH), 7.08 (2H, t, J = 7.7 Hz, Ph-H), 6.97 (2H, d, J = 8 Hz, Ph-H), 6.87 (2H, d, J = 8 Hz, Ph-H), 6.45 (1H, d, J = 8 Hz, Ph-H), 5.07 (1H, dd, J = 11.7, 6.6 Hz, CHCO), 4.54 (1H, q, J = 7.3 Hz, CHN), 4.43 (1H, t, J = 11.0 Hz, CHPh), 3.22 (1H, d, J = 4.4 Hz), 2.16–0.83 (12 H, m, aliphatic C-H); <sup>13</sup>C-NMR (CDCl<sub>3</sub>, 100 MHz): δ = 191.67, 181.97, 154.84, 146.69, 142.54, 139.78, 133.34, 129.39, 128.16, 127.44, 126.93, 125.55, 125.42, 124.12, 122.07, 121.41, 118.44, 112.22, 111.31, 85.63, 85.25, 83.06, 73.14, 57.83, 46.34, 41.88, 40.99, 37.30, 28.55, 28.44, 27.76, 24.73, 23.97; Anal. for C<sub>32</sub>H<sub>29</sub>ClN<sub>4</sub>O<sub>3</sub>; calcd: C, 69.49; H, 5.29; N, 10.13 Exper.: C, 69.55; H, 5.16; N, 10.34.

**2'-(1H-Benzo[d]imidazole-2-carbonyl)-5-chloro-1'-(4-(dimethylamino)phenyl)-1',2',4a',5',6',7',8',8a',9',9a'-decahydrospiro[indoline-3,3'-pyrrolo[1,2-a]indol]-2-one (7j).**

Orange solid; yield (45%); m.p.:140–142 °C; IR (KBr, cm<sup>-1</sup>): 3434 (NH), 3275 (NH), 3094 (CH), 2929 (CH),1729 (CO), 1682 (CO); <sup>1</sup>H-NMR (CDCl<sub>3</sub>, 400 MHz): δ 9.81 (1H, s, NH), 8.01 (1H, s, NH), 7.78 (1H, d, J = 8.0 Hz, Ph-H), 7.31 (5H, m, Ph-H), 7.17 (1H, d, J = 2.2 Hz, Ph-H), 6.94 (1H, dd, J = 8.3, 2.3 Hz, Ph-H), 6.65 (2H, d, J = 8.8 Hz, Ph-H), 6.31 (1H, d, J = 8.6 Hz, Ph-H), 5.32 (1H, d, J = 12.4 Hz, CHCO), 4.38–4.27 (1H, m, CHN), 4.10 (1H, t, J = 7.3 Hz, CHPh), 3.19 (1H, d, J = 3.8 Hz), 2.87 (6H, s, NCH<sub>3</sub>), 2.07–0.83 (12 H, m, aliphatic C-H); <sup>13</sup>C-NMR (CDCl<sub>3</sub>, 100 MHz): δ = 189.78, 181.66, 149.77, 147.05, 139.62, 133.54, 129.10, 128.85, 128.72, 127.56, 126.77, 126.36, 112.88, 110.59, 72.04, 71.13, 65.09, 57.80, 53.18, 40.70, 31.67, 28.50, 27.81, 24.84, 22.74, 19.86; Anal. for C<sub>34</sub>H<sub>34</sub>ClN<sub>5</sub>O<sub>2</sub>; calcd: C, 70.39; H, 5.91; N, 12.07 Exper.: C, 70.65; H, 6.06; N, 11.94.

**2'-(1H-Benzo[d]imidazole-2-carbonyl)-1'-(4-bromophenyl)-5-chloro-1',2',4a',5',6',7',8',8a',9',9a'-decahydrospiro[indoline-3,3'-pyrrolo[1,2-a]indol]-2-one (7k).**

Yellow solid; yield (72%); m.p.:159–161 °C; IR (KBr, cm<sup>-1</sup>): 3625 (NH), 3422 (NH), 3088 (CH), 2913 (CH),1725 (CO), 1682 (CO); <sup>1</sup>H-NMR (CDCl<sub>3</sub>, 400 MHz): δ 10.08 (1H, s, NH), 8.46 (1H, s, NH), 7.80 (1H, d, J = 8.2 Hz, Ph-H), 7.36 (2H, d, J = 8.6 Hz, Ph-H), 7.31–7.16 (7H, m, Ph-H), 6.99–6.93 (1H, m, Ph-H), 6.34 (1H, d, J = 8.2 Hz, Ph-H), 5.30 (1H, d, J = 12.3 Hz, CHCO), 4.36–4.24 (1H, m, CHN), 3.75 (1H, t, J = 12.4 Hz, CHPh), 3.19 (1H, d, J = 3.9 Hz), 2.22–0.82 (12 H, m, aliphatic C-H); <sup>13</sup>C-NMR (CDCl<sub>3</sub>, 100 MHz): δ = 189.58, 181.78, 146.77, 143.06, 139.92, 138.08, 133.72, 131.76, 129.87, 129.35, 127.32, 126.82, 126.65, 126.03, 122.61, 120.92, 112.11, 110.94, 71.97, 71.19, 65.20, 57.78, 53.43, 41.86, 37.41, 28.43, 27.81, 24.78, 19.75; Anal. for C<sub>32</sub>H<sub>28</sub>BrClN<sub>4</sub>O<sub>2</sub>; calcd: C, 62.40; H, 4.58; N, 9.10 Exper.: C, 62.60; H, 4.34; N, 9.03.

**2'-(1H-Benzo[d]imidazole-2-carbonyl)-5-chloro-1'-(3-fluorophenyl)-1',2',4a',5',6',7',8',8a',9',9a'-decahydrospiro[indoline-3,3'-pyrrolo[1,2-a]indol]-2-one (7l).**

Pale yellow solid; yield (42%); m.p.:143–145 °C; IR (KBr, cm<sup>-1</sup>): 3625 (NH), 3422 (NH), 3088 (CH), 2913 (CH),1725 (CO), 1682 (CO); <sup>1</sup>H-NMR (CDCl<sub>3</sub>, 400 MHz): δ 9.51 (1H, s, NH), 7.86 (1H, d, J = 8.0 Hz, Ph-H), 7.42 (1H, s, NH), 7.32 (2H, d, J = 4 Hz, Ph-H), 7.29–7.27 (2H, m, Ph-H), 7.23–7.13 (3H, m, Ph-H), 6.96 (1H, dd, J = 8.5, 2.2 Hz, Ph-H), 6.91–6.85 (1H, m, Ph-H), 6.32 (1H, d, J = 8.4 Hz, Ph-H), 5.31 (1H, d, J = 12.0 Hz, CHCO), 4.41–4.30 (1H, m, CHN), 3.79 (1H, t, J = 12.4 Hz, CHPh), 3.22 (1H, d, J = 4.3 Hz, CHPh), 2.17–0.88 (12 H, m, aliphatic C-H); Anal. for C<sub>32</sub>H<sub>28</sub>ClFN<sub>4</sub>O<sub>2</sub>; calcd: C, 69.25; H, 5.08; N, 10.09 Exper.: C, 69.40; H, 4.94; N, 10.13.

**2'-(1H-Benzo[d]imidazole-2-carbonyl)-5-chloro-1'-(furan-2-yl)-1',2',4a',5',6',7',8',8a',9',9a'-decahydrospiro[indoline-3,3'-pyrrolo[1,2-a]indol]-2-one (7m).**

Pale yellow solid; yield (62%); m.p.:165–167 °C; IR (KBr,  $\text{cm}^{-1}$ ): 3435 (NH), 3256 (NH), 3090 (CH), 2928 (CH),1729 (CO), 1687 (CO);  $^1\text{H-NMR}$  ( $\text{CDCl}_3$ , 400 MHz):  $\delta$  10.31 (1H, s, NH), 8.77 (1H, s, NH), 7.83 (1H, d,  $J = 8$  Hz, Ph-H), 7.36 (1H, d,  $J = 8$  Hz, Ph-H), 7.28 (1H, t,  $J = 7.5$  Ph-H), 7.22 (2H, d,  $J = 7.9$  Hz, Ar), 7.11 (1H, s, Ph-H), 6.93 (1H, d,  $J = 8.7$  Hz, Ph-H), 6.39 (1H, d,  $J = 8.7$  Hz, Ph-H), 6.20 (1H, t,  $J = 1.6$  Hz, fur-H), 6.12 (1H, d,  $J = 3.6$  Hz, fur-H), 5.37 (1H, d,  $J = 12.3$  Hz,  $\text{CHCO}$ ), 4.39 (1H, q,  $J = 8.3$  Hz,  $\text{CHN}$ ), 3.97 (1H, t,  $J = 11.4$  Hz,  $\text{CHPh}$ ), 3.17 (1H, d,  $J = 4.4$  Hz), 2.16–0.85 (12 H, m, aliphatic C-H);  $^{13}\text{C-NMR}$  ( $\text{CDCl}_3$ , 100 MHz):  $\delta = 189.68, 181.80, 153.04, 146.83, 143.19, 141.75, 141.71, 141.67, 139.98, 133.89, 129.32, 127.40, 126.74, 126.63, 125.97, 123.69, 122.69, 112.20, 111.05, 110.27, 106.01, 71.94, 68.30, 62.85, 57.68, 46.89, 41.94, 37.74, 28.39, 27.79, 24.80, 19.69$ ; Anal. for  $\text{C}_{30}\text{H}_{27}\text{ClN}_4\text{O}_3$ ; calcd: C, 68.37; H, 5.16; N, 10.63 Exper.: C, 68.60; H, 4.94; N, 10.33.

**2'-(1H-Benzo[d]imidazole-2-carbonyl)-5-chloro-1'-(4-nitrophenyl)-1',2',4a',5',6',7',8',8a',9',9a'-decahydrospiro[indoline-3,3'-pyrrolo[1,2- a]indol]-2-one (7n).**

Pale yellow solid; yield (46%); m.p.:165–167 °C; IR (KBr,  $\text{cm}^{-1}$ ): 3437 (NH), 3255 (NH), 3094 (CH), 2929 (CH),1728 (CO), 1686 (CO);  $^1\text{H-NMR}$  ( $\text{CDCl}_3$ , 400 MHz):  $\delta$  9.81 (1H, s, NH), 8.12 (1H, s, NH), 8.12 (2H, d,  $J = 8.6$  Hz, Ph-H), 7.80 (1H, d,  $J = 8.0$  Hz, Ph-H), 7.63 (2H, d,  $J = 8.6$  Hz, Ph-H), 7.33–7.23 (3H, m, Ph-H), 7.14 (1H, s, Ph-H), 6.97 (1H, dd,  $J = 8.3, 1.8$  Hz, Ph-H), 6.36 (1H, d,  $J = 8.6$  Hz, Ph-H), 5.35 (1H, d,  $J = 11.9$  Hz,  $\text{CHCO}$ ), 4.41–4.35 (1H, m,  $\text{CHN}$ ), 3.90 (1H, t,  $J = 12$  Hz,  $\text{CHPh}$ ), 3.23 (1 H, d,  $J = 3.9$  Hz), 2.03– 0.84 (12 H, m, aliphatic C-H);  $^{13}\text{C-NMR}$  ( $\text{CDCl}_3$ , 100 MHz):  $\delta = 189.08, 181.27, 147.16, 146.89, 146.55, 143.00, 139.84, 133.60, 129.53, 129.10, 129.04, 126.98, 126.86, 125.72, 123.92, 122.54, 112.06, 110.85, 71.90, 71.25, 65.46, 57.83, 53.73, 41.86, 37.38, 31.67, 28.38, 27.80, 24.73, 23.95$ ; Anal. for  $\text{C}_{32}\text{H}_{28}\text{ClN}_5\text{O}_4$ ; calcd: C, 66.03; H, 4.85; N, 12.03 Exper.: C, 66.10; H, 4.74; N, 12.11.

**2'-(1H-benzo[d]imidazole-2-carbonyl)-5-chloro-1'-(3-nitrophenyl)-1',2',4a',5',6',7',8',8a',9',9a'-decahydrospiro[indoline-3,3'-pyrrolo[1,2- a]indol]-2-one (7o).**

Pale yellow solid; yield (52%); m.p.:135–137 °C; IR (KBr,  $\text{cm}^{-1}$ ): 3438 (NH), 3257 (NH), 3092 (CH), 2930 (CH),1729 (CO), 1688 (CO);  $^1\text{H-NMR}$  ( $\text{CDCl}_3$ , 400 MHz):  $\delta$  9.55 (1H, s, NH), 8.36 (1H, s, NH), 8.06 (1H, dd,  $J = 8.1, 2.3$  Hz, Ph-H), 7.86 (2H, d,  $J = 8.2$  Hz, Ph-H), 7.57 (1H, s, Ph-H), 7.47 (1H, t,  $J = 8$  Hz, Ph-H), 7.31 (3H, d,  $J = 4.0$  Hz, Ph-H), 7.14 (1H, d,  $J = 2.1$  Hz, Ph-H), 6.98 (1H, dd,  $J = 8.3, 2.4$  Hz, Ph-H), 6.33 (1H, d,  $J = 8.0$  Hz, Ph-H), 5.31 (1H, d,  $J = 12.0$  Hz,  $\text{CHCO}$ ), 4.46–4.36 (1H, m,  $\text{CHN}$ ), 3.92 (1H, t,  $J = 12.0$  Hz,  $\text{CHPh}$ ), 3.24 (1H, d,  $J = 4.3$  Hz), 2.19–0.81 (12 H, m, aliphatic C-H); Anal. for  $\text{C}_{32}\text{H}_{28}\text{ClN}_5\text{O}_4$ ; calcd: C, 66.03; H, 4.85; N, 12.03 Exper.: C, 66.09; H, 4.73; N, 12.10.

### 2.3. NCI Screening

The compounds have been processed according to the standard method NCI-60 Human Tumor Cell Lines Screen for the organic compound at the development therapeutic program (DTP) (see Supplementary Materials, Table S2; Figures S1 and S2).

### 2.4. Anticancer Activity Protocol

The anticancer activity protocol was carried out according to the method reported in [48]. “The cytotoxicity of tested compounds was investigated on a human normal lung fibroblast (Wi-38) cell line, triple-negative breast (MDA-MB 231) cells, and prostate cancer (PC3) cells. These cells were cultured in DMEM containing 10% fetal bovine serum. After cell seeding (10,000, 4000, and 5000 cells, respectively, per well) in 96-well cell culture plates and incubating for 24 h in a 5%  $\text{CO}_2$  incubator, serial dilutions (2,4,6,8, and 10  $\mu\text{M}$ ) of the tested compounds were added. Following 48 h in a 5%  $\text{CO}_2$  incubator, 20  $\mu\text{L}$  of MTT (5 mg/mL) was added and incubated for 4 h, then this solution was removed and 100  $\mu\text{L}$  of DMSO was added. The absorbance was measured at 590 nm (BMG LabTech, Ortenberg, Germany). The half-inhibitory growth concentration ( $\text{IC}_{50}$ ) was calculated by GraphPad Prism software” [48].

### 2.5. MDM2 Binding Analysis by Microscale Thermophoresis (MST) Assay

The full protocol has been provided in SI and the binding curve is shown in the Supplementary Material (Figures S3–S6).

### 2.6. Methodology for Molecular Docking

Two-dimensional structures of compounds **7a**, **7g**, **7h**, and **7k** were drawn via the builder and subjected to preliminary structure preparation, namely energy minimization with the force field MMFF94x and the subsequent application of partial charges. The X-Ray crystal structure of MDM2 with PDB ID: 5LAZ, having a cocrystallized ligand with structural similarity to the studied compounds, was retrieved from the RCSB Protein Data Bank for the docking studies. Structure preparation of the protein was brought about by energy minimization with force field Amber10:EHT and partial charges were then applied to the protein. The cocrystallized ligand (6ST), after the necessary structure preparations, was used as a reference compound for validation of the results in docking studies of the aforementioned compounds [34]. Benchmarking of the docking protocols was performed well before the docking studies. Redocking of the 6ST ligand was brought about to observe the deviation of the ligand conformation from the original one (SI Figure S7). All the operations were performed in the molecular operating environment (MOE 2019.01) [49], which was chosen based on the RMSD value (0.14 Å) between the coordinates of the cognate ligand and the simulated pose. Induced fit docking was directed to the ligand atoms, brought about by placement of the ligand into the binding site of MDM2 utilizing the triangle matcher algorithm followed by determining the scores of the generated fifteen conformations through the London dG scoring function. Finally, five top-scored conformations were retained and evaluated by the GBVI/WSA dG scoring function. Thereafter, the same protocols were followed for the docking simulation of the studied compounds. The interaction patterns of the ligands with binding site residues were analyzed by the Protein-Ligand Interaction Profiler [50].

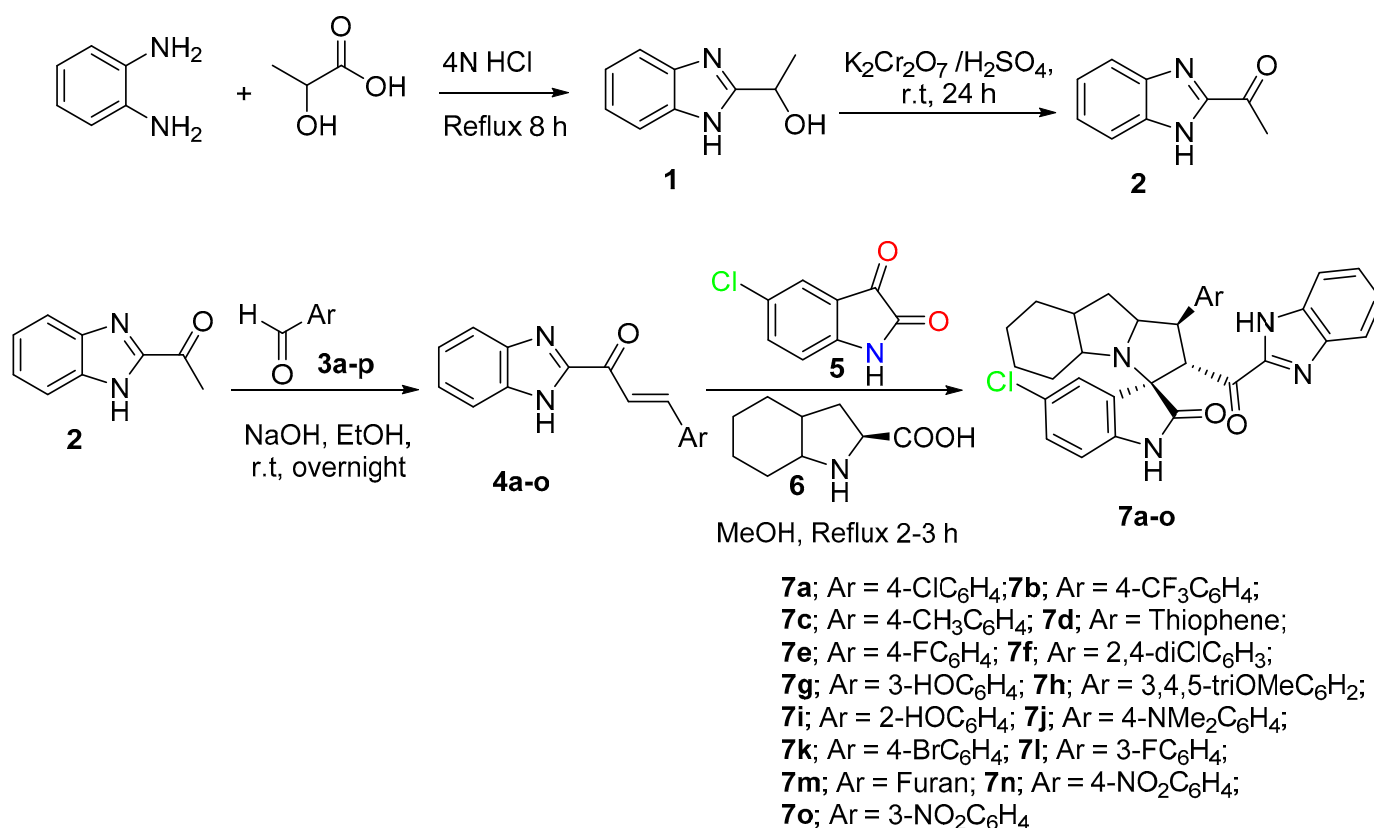
### 2.7. Statistical Analysis

The data are expressed as mean  $\pm$  standard error of the mean (SEM) and values were considered significantly different at  $p < 0.05$ , using one-way analysis of variance (ANOVA) and Tukey's test (SPSS software version 16).

## 3. Results and Discussion

### 3.1. Chemistry

Based on the recently published idea of spiroxindole having the benzimidazole nucleus and showing promising results against cancer cell lines and an antimetastatic effect. To study the cytotoxicity and structure reactivity relationship, a new library **7a-o** has been synthesized and characterized (Scheme 1). Different electronic effects on the aromatic ring, including electron-donating and electron-withdrawing effects, also achieved a heterocycle aromatic ring and were explored. The synthetic methodology was carried out based on a multicomponent one-pot reaction *via* the [3+2] cycloaddition reaction approach [48]. The desired dipolarphiles were synthesized from orthophenylene diamine in a consequential step. Mixing the chalcones **4a-o** with the 5-chloroisatin, **5** and the key amino acid **6** in methanol under reflux for 2–3 h, afforded the final compounds in a high chemical yield and a regio- and diastereo-selective manner. The stereochemistry for the final cycloadduct is matched with the previous lead compound published by our research group [48].



**Scheme 1.** Synthetic methodology for the desired spirooxindole derivative **7a-o**.

### 3.2. In Vitro Anti-Cancer Activity Assays

#### 3.2.1. NCI Screening (Development Therapeutic Program, DTP)

The successfully synthesized spirooxindoles (**7a-o**) were submitted for NCI for screening against 60 various cancer cell lines, classified into nine subpanels: breast, kidney, melanoma colon, prostate, CNS, ovary, melanoma, leukemia, and lung cancers. The initial single dose assay for the assessed spirooxindoles were tested at a 10  $\mu$ M and the results were then expressed as a percentage of growth inhibition (GI%) (Table S2). As observed, the synthesized compounds inhibited the growth of the NCI cell-line panel according to the following order: breast > renal > leukemia cancer cell lines > other tested cancer cell lines (Table S2). The initial results afforded the most active compound, **7g**, which entered the five dose assays, and the results are shown in Supporting Materials (Figures S1 and S2).

#### 3.2.2. MTT Assay

In order to determine the IC<sub>50</sub> ( $\mu$ M) of the synthesized spirooxindoles, **7a-o** were subjected to an MTT assay in vitro against the two-cancer cell line MDA-MB 231 and PC3 cells, and the data reported in Table 1. For the breast cancer line (MDA-MB 231) the compounds are shown in IC<sub>50</sub> ( $\mu$ M) in the range between 3.797–6.879  $\mu$ M; the most active candidate between the series was compound **7d** with IC<sub>50</sub> = 3.797  $\pm$  0.205  $\mu$ M, the chemical structure compromises a thiophene ring. On the other hand, the least reactivity was compound **7n** with IC<sub>50</sub> = 6.879  $\pm$  0.308  $\mu$ M. All other compounds are shown in the range of 4  $\mu$ M reactivity. In the case of prostate cancer (PC3), the reactivity of the synthesized compounds exhibited the range of IC<sub>50</sub> = 4.252 to 7.567  $\mu$ M. In the case of compound **7a** with the Cl-atom in the fourth position showed IC<sub>50</sub> = 4.763  $\pm$  0.069 and 4.574  $\pm$  0.011  $\mu$ M, for both tested two-cancer cells MDA-MB 231, and PC3, respectively. The reactivity slightly improved compared with compound **7a** when the CF<sub>3</sub>-group was introduced into the aromatic ring, as indicated in compound **7b** which showed IC<sub>50</sub> = 4.284  $\pm$  0.007 and 4.404  $\pm$  0.008  $\mu$ M; **7e** contain the *p*-fluoro atom on the aromatic ring compared



with **7l** having the *m*-fluoro atom on the aromatic, where no differences were observed in the cytotoxicity. In the isosteric analog of the compound **7d**, which replaced the thiophene with furan heterocycle, as shown in compound **7m**, the cytotoxicity dropped to  $IC_{50} = 6.039 \pm 0.111$  and  $5.098 \pm 0.119 \mu\text{M}$  with less than 1.6 and 1.18 times, compared to the compound **7d**. Introducing the electron-withdrawing effect of the  $\text{NO}_2$  group either in the *para*- or *meta*-position, we observed that  $\text{NO}_2$  in the *meta* (compound **7o**) was more active than the *para*-position (compound **7n**) with 1.66 and 1.77 folds. The existence of electron donating groups such as methyl group (compound **7c**); hydroxyl group (compound **7g** or compound **7e**); trimethoxy groups (compound **7h**); and dimethyl amine (compound **7j**) did not alter the reactivity.

**Table 1.** The estimated  $IC_{50}$  ( $\mu\text{M}$ ) of **7a–o** on Wi-38 viability, the growth of MDA-MB 231, and PC3 cells.

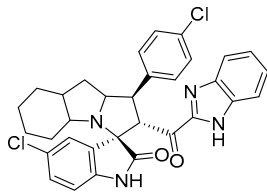
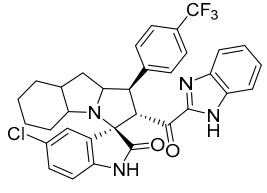
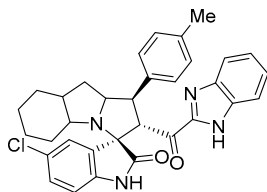
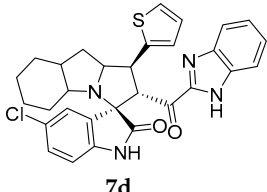
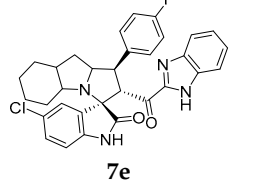
Chemical Structure	Wi-38	MDA-MB 231	PC3
	$IC_{50}$ ( $\mu\text{M}$ )		
 <p><b>7a</b></p>	$5.178 \pm 0.333$	$4.763 \pm 0.069$	$4.574 \pm 0.011$
 <p><b>7b</b></p>	$5.157 \pm 0.039$	$4.284 \pm 0.007$	$4.404 \pm 0.008$
 <p><b>7c</b></p>	$4.466 \pm 0.088$	$4.221 \pm 0.070$	$4.504 \pm 0.059$
 <p><b>7d</b></p>	$4.325 \pm 0.062$	$3.797 \pm 0.205$	$4.314 \pm 0.036$
 <p><b>7e</b></p>	$4.024 \pm 0.011$	$4.143 \pm 0.164$	$4.252 \pm 0.128$

Table 1. Cont.

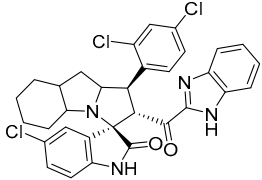
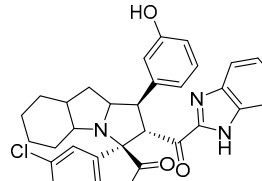
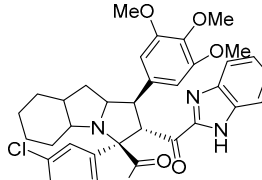
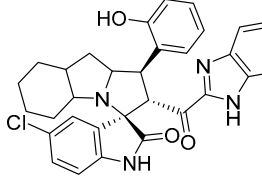
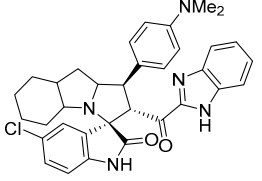
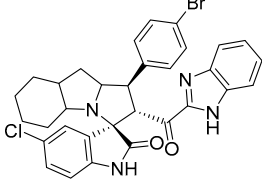
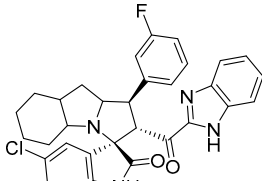
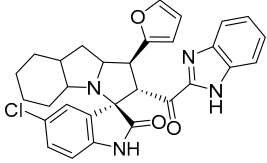
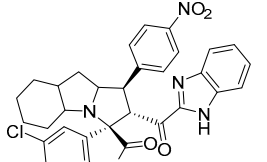
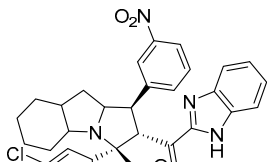
Chemical Structure	Wi-38	MDA-MB 231		PC3
		IC <sub>50</sub> (μM)		
 <p><b>7f</b></p>	5.084 ± 0.152	4.274 ± 0.167	4.388 ± 0.008	
 <p><b>7g</b></p>	5.120 ± 0.115	4.329 ± 0.163	4.294 ± 0.023	
 <p><b>7h</b></p>	4.938 ± 0.161	4.261 ± 0.095	4.241 ± 0.045	
 <p><b>7i</b></p>	4.854 ± 0.009	4.371 ± 0.174	4.495 ± 0.034	
 <p><b>7j</b></p>	4.267 ± 0.153	4.261 ± 0.079	4.420 ± 0.008	
 <p><b>7k</b></p>	4.316 ± 0.007	4.479 ± 0.313	4.539 ± 0.094	
 <p><b>7l</b></p>	4.401 ± 0.092	4.156 ± 0.135	4.360 ± 0.208	

Table 1. Cont.

Chemical Structure	Wi-38	MDA-MB 231	PC3
	IC <sub>50</sub> (μM)		
 7m	4.698 ± 0.129	6.039 ± 0.111	5.098 ± 0.119
 7n	3.959 ± 0.046	6.879 ± 0.308	7.567 ± 0.709
 7o	5.187 ± 0.089	4.138 ± 0.186	4.275 ± 0.005

All values are presented as mean ± SEM.

### 3.2.3. Microscale Thermophoresis Assay (MST) for MDM2 Binding Detection

Compounds **7a**, **7g**, **7h**, and **7k** shown very good anti-cancer potential as well as high safety profiles as obtained by the MTT assay. Accordingly, the compound **7a**, **7g**, **7h**, and **7k** were then tested for MDM2 binding analysis. The tested compound was incubated with a fluorescently labeled MDM2 at increasing concentrations (0.763 nM to 25 μM; Solubility play a crucial role to reach maximum concentration). MST binding curves showed that spirooxindole-based benzimidazole **7a**, **7g**, and **7h** showed moderate binding affinity in the range of ( $K_D$ ; 2.38–38 μM). Compound **7a** showed better binding reactivity compared to our previous spirooxindole-based benzimidazole, which has been shown ( $K_D$ ; 7.94 μM) [48]. The **7k** did not show any binding detection (Table 2).

Table 2. MST binding assay results of MDM2.

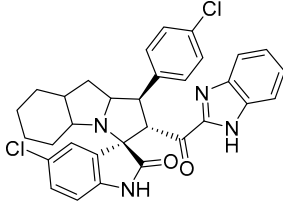
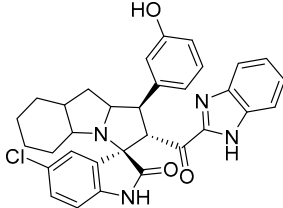
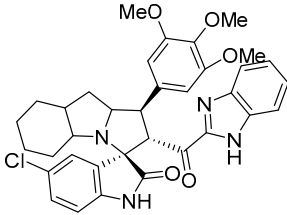
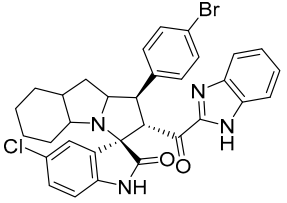
#	Code	Chemical Structures	K <sub>D</sub> (μM)
1	7a		2.38
2	7g		38

Table 2. Cont.

#	Code	Chemical Structures	KD ( $\mu\text{M}$ )
3	7h		10.6
4	7k		No binding detected

### 3.3. Molecular Docking of the Studied Compound

Results of the docking simulations of the spirooxindoles molecules were validated relative to the reference compound (6ST), which was firmly held into the binding site by a diverse network of interactions. The nitrogen of the imidazole ring of His96 and oxygen in the carboxylic acid moiety of Leu54 accepted hydrogens from the N-H of indolinone and the N-H of pyrrolidine rings, resulting in hydrogen bonds with 1.99 Å and 2.16 Å lengths, respectively. Additionally, His96 had  $\pi$ -stacking and halogen bonding with the chloroindolinone moiety. There were formed salt bridges by the carboxylate group of this compound with His73 and Lys94. This binding was further enhanced by hydrophobic interactions with seven amino acid residues.

Compound 7a developed a network of interactions similar to that of the reference compound. A hydrogen bond was established with the ligand at a distance of 2.08 Å, where hydrogen was donated by the N-H of benzimidazole to Leu54. Furthermore, His96 formed  $\pi$ -stacking and halogen bonding with the chlorobenzene ring the same way it was created with the reference compound. Similarly, hydrophobic interactions formed by seven residues well accommodated this compound into the binding site. In contrast to 7a, compound 7g formed two hydrogen bonds. One of the hydrogen bonds between benzimidazole moiety and Val93 was of 3.02 Å length, and the other bond resulted between the amino group of Lys96, being the donor, and phenolic group of the ligand was accepting at 2.59 Å distance. His96 provided  $\pi$ -stacking with the aromatic rings of benzimidazole moiety. However, fewer hydrophobic interactions were observed for this compound as compared to 7a. In the case of 7h, only one hydrogen bond was formed, which was between the amino group of Lys94 and the central methoxy group of the trimethoxybenzene substituent in the compound. The benzimidazole of this compound was anchored by  $\pi$ -stacking, twice with His96 and once with Tyr100. Three hydrophobic interactions were also developed. For compound 7k, the observed interactions included a halogen bond between its bromobenzene substituent and His96, and hydrophobic interactions with six residues of the MDM2 binding site.

The docked poses of the studied compounds are presented in Figure 2, and Table 3 enlists all the observed interactions, the interacting groups, and docking scores.

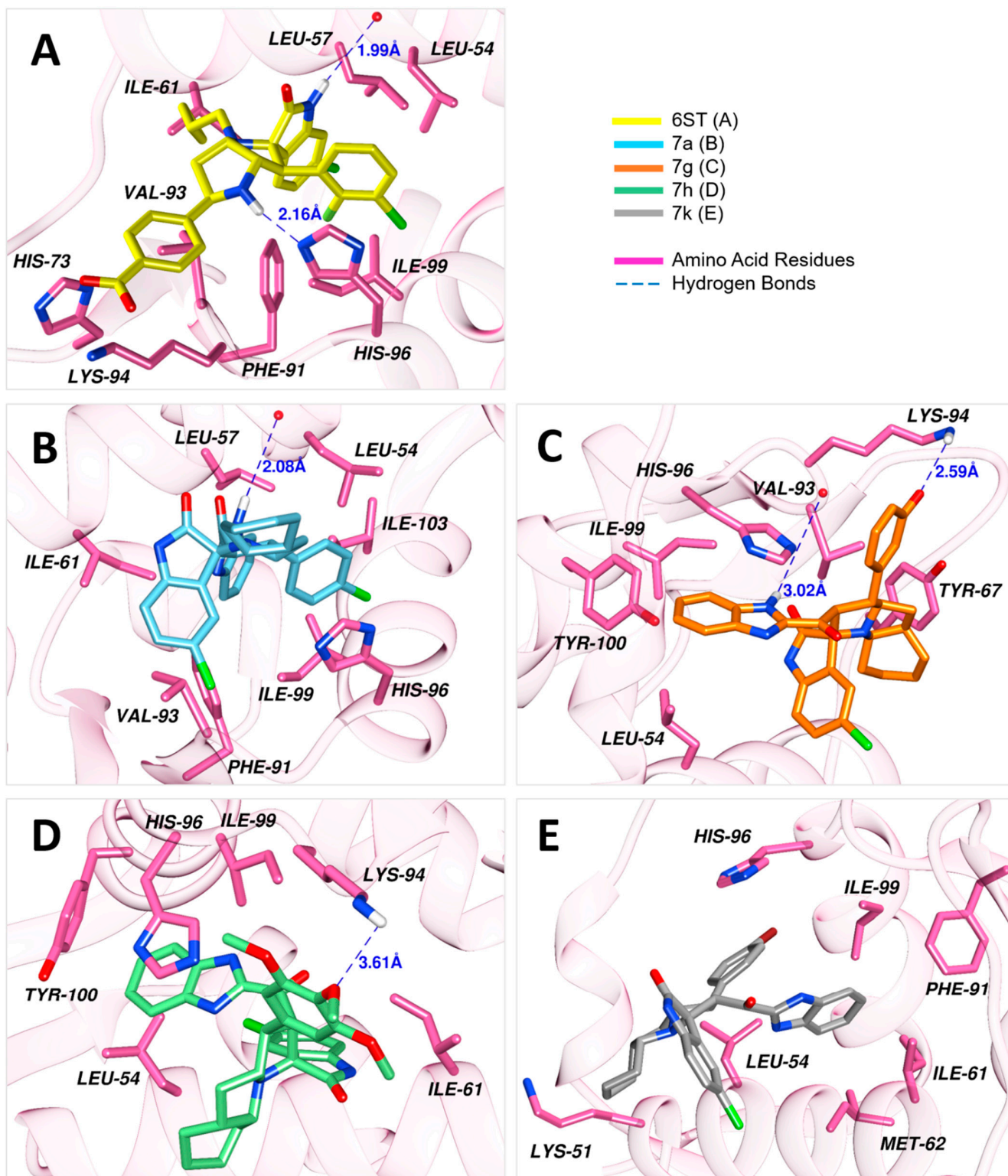


Figure 2. Docked conformations of the ligands into the binding site of MDM2 (PDB ID: 5LAZ).

**Table 3.** Docking scores and network of interactions formed between the ligands and residues of MDM2.

Cpd. ID	S (kcal/mol)	Hydrogen Bonding			Hydrophobic Interactions	Other Interactions
		Residues	Ligand Residues	Distance (Å)		
7a	−7.05	Leu54	N-H of benzimidazole	2.08	Leu54, Leu57, Ile61, Phe91, Val93, Ile99, Ile103	$\pi$ -stacking, Halogen bonding with His96
7g	−7.09	Val93	N-H of benzimidazole	3.02	Leu54, Tyr67, Ile99, Tyr100	$\pi$ -stacking with His96
		Lys94	O of phenol ring	2.59		
7h	−7.43	Lys94	O of methoxy	3.29	Leu54, Ile61, Ile99	$\pi$ -stacking with His96, Tyr100
7k	−7.29	-	-	-	Lys51, Leu54, Leu57, Ile61, Phe91, Ile99	halogen bonding with His96
6ST	−8.97	Leu54	N-H of indolinone	1.99	Leu54, Leu57, Ile61, Phe91, Val93, Lys94, Ile99	$\pi$ -stacking, Halogen bonding with His96; salt bridge with His73, Lys94
		His96	N-H of pyrrolidine	2.16		

#### 4. Conclusions

New spiroxindoles, combined with a benzimidazole scaffold, were synthesized, characterized, and identified as an MDM2 inhibitor. The requisite spiroxindoles were successfully achieved *via* the [3+2] cycloaddition reaction approach, which separated in an excellent regioselective and diastereoselective manner. The separated spiroxindoles showed promising results against cancer cells including MDA-MB 231 and PC3 in microscale reactivity. The anticancer reactivity for compound **7d** showed potential activity with  $IC_{50} = 3.797 \pm 0.205 \mu\text{M}$  and was recognized as the most active candidate in the series. MDM2 binding analysis showed that compound **7a** could be inhibited by the MDM2 with  $K_D = 2.38 \mu\text{M}$ . This finding could be of possible use for cancer research development in the future.

**Supplementary Materials:** The following supporting information can be downloaded at: <https://www.mdpi.com/article/10.3390/separations10040225/s1>, Figure S1: one dose for compound **7g**; Figure S2: Five doses for the compound **7g**; Figure S3–S6: Binding curve for MST assay; Figure S7: validation of the docking protocol. Figure S8–S38: Selected NMR and IR spectrum; Table S1: Characterization of the chalcones **4a–o**; Table S2: GI % at 10  $\mu\text{M}$  concentration for compounds **7a–o**; Table S3: The percentage of Wi-38 viability and the toxicity percentage of MDA-MB231, and PC3 cells after incubation with 5  $\mu\text{M}$  of different tested compounds (**7a–o**).

**Author Contributions:** Conceptualization, A.B. and A.D.; methodology, S.A., M.A. and A.S.A.; software, M.S. and Z.U.-H.; validation, S.A., M.A. and A.S.A.; formal analysis, S.A., M.A. and A.S.A.; investigation, S.A., M.A. and A.S.A.; resources, A.B.; data curation, S.A. and Z.U.-H.; Biological activity assays: A.D. and M.M.A.-S.; writing—original draft preparation, A.B.; writing—review and editing, A.B.; visualization, A.M.A.-M.; supervision, A.M.A.-M.; project administration, M.A.; funding acquisition, A.B. All authors have read and agreed to the published version of the manuscript.

**Funding:** The authors extend their appreciation to the Deputyship for Research & Innovation, Ministry of Education in Saudi Arabia for funding this research work through the project number (IFKSURG–2-361).

**Institutional Review Board Statement:** Not applicable.

**Informed Consent Statement:** Not applicable.

**Data Availability Statement:** Not applicable.

**Acknowledgments:** The authors extend their appreciation to the Deputyship for Research & Innovation, Ministry of Education in Saudi Arabia for funding this research work through the project number (IFKSURG–2-361).

**Conflicts of Interest:** The authors declare no conflict of interest.

## References

1. Xue, P.; Zhang, Z.; Sun, S. Targeting p53-MDM2 Interaction by Small Molecule Inhibitors: A Promising Strategy for Cancer Treatment. *Int. J. Mol. Sci.* **2019**, *20*, 64.
2. Masuda, H.; Takahashi, M.; Takahashi, R. Small-molecule inhibitors targeting the p53-MDM2 interaction for cancer therapy. *Drug Discov. Today* **2018**, *23*, 774–784.
3. Zhou, X.; Xu, X.; Huang, P. Small-molecule inhibitors targeting the p53-MDM2 interaction for cancer therapy: A review. *Bioorg. Med. Chem.* **2016**, *24*, 4710–4717.
4. Zhu, H.; Gao, H.; Ji, Y.; Zhou, Q.; Du, Z.; Tian, L.; Jiang, Y.; Yao, K.; Zhou, Z. Targeting p53–MDM2 interaction by small-molecule inhibitors: Learning from MDM2 inhibitors in clinical trials. *J. Hematol. Oncol.* **2022**, *15*, 91. [[CrossRef](#)]
5. Zhuang, C.; Miao, Z.; Zhu, L.; Dong, G.; Guo, Z.; Wang, S.; Zhang, Y.; Wu, Y.; Yao, J.; Sheng, C.; et al. Discovery, synthesis, and biological evaluation of orally active pyrrolidone derivatives as novel inhibitors of p53-MDM2 protein-protein interaction. *J. Med. Chem.* **2012**, *55*, 9630–9642. [[CrossRef](#)]
6. Ding, K.; Lu, Y.; Nikolovska-Coleska, Z.; Wang, G.; Qiu, S.; Shangary, S.; Gao, W.; Qin, D.; Stuckey, J.; Krajewski, K.; et al. Structure-based design of spiro-oxindoles as potent, specific small-molecule inhibitors of the MDM2-p53 interaction. *J. Med. Chem.* **2006**, *49*, 3432–3435. [[CrossRef](#)]
7. Sanz, G.; Singh, M.; Peugeot, S.; Selivanova, G. Inhibition of p53 inhibitors: Progress, challenges and perspectives. *J. Mol. Cell Biol.* **2019**, *11*, 586–599. [[CrossRef](#)]
8. Zhang, Q.; Zeng, S.X.; Lu, H. Targeting p53-MDM2-MDMX loop for cancer therapy. In *Mutant p53 and MDM2 in Cancer*; Springer: Berlin/Heidelberg, Germany, 2014; pp. 281–319.
9. Ding, K.; Lu, Y.; Nikolovska-Coleska, Z.; Qiu, S.; Ding, Y.; Gao, W.; Stuckey, J.; Krajewski, K.; Roller, P.P.; Tomita, Y.; et al. Structure-based design of potent non-peptide MDM2 inhibitors. *J. Am. Chem. Soc.* **2005**, *127*, 10130–10131. [[CrossRef](#)]
10. Fry, D.C.; Emerson, S.D.; Palme, S.; Vu, B.T.; Liu, C.M.; Podlaski, F. NMR structure of a complex between MDM2 and a small molecule inhibitor. *J. Biomol. NMR* **2004**, *30*, 163–173. [[CrossRef](#)]
11. Rothweiler, U.; Czarna, A.; Krajewski, M.; Ciombor, J.; Kalinski, C.; Khazak, V.; Ross, G.; Skobeleva, N.; Weber, L.; Holak, T.A. Isoquinolin-1-one inhibitors of the MDM2-p53 interaction. *Chem. Med. Chem.* **2008**, *3*, 1118–1128. [[CrossRef](#)]
12. Kumar, S.K.; Hager, E.; Pettit, C.; Gurulingappa, H.; Davidson, N.E.; Khan, S.R. Design, Synthesis, and Evaluation of Novel Boronic-Chalcone Derivatives as Antitumor Agents. *J. Med. Chem.* **2003**, *46*, 2813–2815. [[CrossRef](#)]
13. Surmiak, E.; Twarda-Clapa, A.; Zak, K.M.; Musielak, B.; Tomala, M.D.; Kubica, K.; Grudnik, P.; Madej, M.; Jablonski, M.; Potempa, J.; et al. A Unique Mdm2-Binding Mode of the 3-Pyrrolin-2-one- and 2-Furanone-Based Antagonists of the p53-Mdm2 Interaction. *ACS Chem. Biol.* **2016**, *11*, 3310–3318. [[CrossRef](#)]
14. Yang, M.C.; Peng, C.; Huang, H.; Yang, L.; He, X.H.; Huang, W.; Cui, H.L.; He, G.; Han, B. Organocatalytic Asymmetric Synthesis of Spiro-oxindole Piperidine Derivatives That Reduce Cancer Cell Proliferation by Inhibiting MDM2-p53 Interaction. *Org. Lett.* **2017**, *19*, 6752–6755. [[CrossRef](#)]
15. Gonzalez, A.Z.; Eksterowicz, J.; Bartberger, M.D.; Beck, H.P.; Canon, J.; Chen, A.; Chow, D.; Duquette, J.; Fox, B.M.; Fu, J.; et al. Selective and potent morpholinone inhibitors of the MDM2-p53 protein-protein interaction. *J. Med. Chem.* **2014**, *57*, 2472–2488. [[CrossRef](#)]
16. Furet, P.; Chene, P.; De Pover, A.; Valat, T.S.; Lisztwan, J.H.; Kallen, J.; Masuya, K. The central valine concept provides an entry in a new class of non peptide inhibitors of the p53-MDM2 interaction. *Bioorg. Med. Chem. Lett.* **2012**, *22*, 3498–3502. [[CrossRef](#)]
17. Koblisch, H.K.; Zhao, S.; Franks, C.F.; Donatelli, R.R.; Tominovich, R.M.; LaFrance, L.V.; Leonard, K.A.; Gushue, J.M.; Parks, D.J.; Calvo, R.R.; et al. Benzodiazepinedione inhibitors of the Hdm2:p53 complex suppress human tumor cell proliferation in vitro and sensitize tumors to doxorubicin in vivo. *Mol. Cancer Ther.* **2006**, *5*, 160–169. [[CrossRef](#)]
18. Pettersson, M.; Quant, M.; Min, J.; Iconaru, L.; Kriwacki, R.W.; Waddell, M.B.; Guy, R.K.; Luthman, K.; Grotli, M. Design, Synthesis and Evaluation of 2,5-Diketopiperazines as Inhibitors of the MDM2-p53 Interaction. *PLoS ONE* **2015**, *10*, e0137867. [[CrossRef](#)]
19. Allen, J.G.; Bourbeau, M.P.; Wohlhieter, G.E.; Bartberger, M.D.; Michelsen, K.; Hungate, R.; Gadwood, R.C.; Gaston, R.D.; Evans, B.; Mann, L.W.; et al. Discovery and optimization of chromenotriazolopyrimidines as potent inhibitors of the mouse double minute 2-tumor protein 53 protein-protein interaction. *J. Med. Chem.* **2009**, *52*, 7044–7053. [[CrossRef](#)]
20. Aguilar, A.; Lu, J.; Liu, L.; Du, D.; Bernard, D.; McEachern, D.; Przybranowski, S.; Li, X.; Luo, R.; Wen, B.; et al. Discovery of 4-((30R,40S,50R)-6''-Chloro-40-(3-chloro-2-fluorophenyl)-10-ethyl-2''-oxodispiro[cyclohexane-1,20pyrrolidine-30,3''-indoline]-50-carboxamido)bicyclo[2.2.2]octane-1-carboxylic Acid (AA-115/APG-115): A Potent and Orally Active Murine Double Minute 2 (MDM2) Inhibitor in Clinical Development. *J. Med. Chem.* **2017**, *60*, 2819–2839.
21. De Jonge, M.; de Weger, V.A.; Dickson, M.A.; Langenberg, M.; Le Cesne, A.; Wagner, A.J.; Hsu, K.; Zheng, W.; Mace, S.; Tuffal, G.; et al. A phase I study of SAR405838, a novel human double minute 2 (HDM2) antagonist, in patients with solid tumours. *Eur. J. Cancer* **2017**, *76*, 144–151. [[CrossRef](#)]
22. Zanjirband, M.; Edmondson, R.J.; Lunec, J. Pre-clinical efficacy and synergistic potential of the MDM2-p53 antagonists, Nutlin-3 and RG7388, as single agents and in combined treatment with cisplatin in ovarian cancer. *Oncotarget* **2016**, *7*, 40115–40134. [[CrossRef](#)] [[PubMed](#)]
23. Novartis Pharmaceuticals. Study of Safety and Efficacy of HDM201 in Combination with LEE011 in Patients with Liposarcoma. ClinicalTrials. Gov Identifier: NCT02343172. 2015. Available online: <https://clinicaltrials.gov/ct2/show/NCT02343172> (accessed on 13 February 2023).

24. Andreeff, M.; Kelly, K.R.; Yee, K.; Assouline, S.; Strair, R.; Popplewell, L.; Bowen, D.; Martinelli, G.; Drummond, M.W.; Vyas, P.; et al. Results of the Phase I Trial of RG7112, a Small-Molecule MDM2 Antagonist in Leukemia. *Clin. Cancer Res.* **2016**, *22*, 868–876. [[CrossRef](#)] [[PubMed](#)]
25. Sun, D.; Li, Z.; Rew, Y.; Gribble, M.; Bartberger, M.D.; Beck, H.P.; Canon, J.; Chen, A.; Chen, X.; Chow, D.; et al. Discovery of AMG 232, a potent, selective, and orally bioavailable MDM2-p53 inhibitor in clinical development. *J. Med. Chem.* **2014**, *57*, 1454–1472. [[CrossRef](#)] [[PubMed](#)]
26. Zhao, Y.; Liu, L.; Sun, W.; Lu, J.; McEachern, D.; Li, X.; Yu, S.; Bernard, D.; Ochsenein, P.; Ferey, V.; et al. Diastereomeric spirooxindoles as highly potent and efficacious MDM2 inhibitors. *J. Am. Chem. Soc.* **2013**, *135*, 7223–7234. [[CrossRef](#)]
27. Tovar, C.; Graves, B.; Packman, K.; Filipovic, Z.; Xia, B.H.M.; Tardell, C.; Garrido, R.; Lee, E.; Kolinsky, K.; To, K.H.; et al. MDM2 small-molecule antagonist RG7112 activates p53 signaling and regresses human tumors in preclinical cancer models. *Cancer Res.* **2013**, *73*, 2587–2597. [[CrossRef](#)]
28. Beloglazkina, A.; Zyk, N.; Majouga, A.; Beloglazkina, E. Recent small-molecule inhibitors of the p53–MDM2 protein–protein interaction. *Molecules* **2020**, *25*, 1211. [[CrossRef](#)]
29. Riedinger, C.; McDonnell, J.M. Inhibitors of MDM2 and MDMX: A structural perspective. *Future Med. Chem.* **2009**, *1*, 1075–1094. [[CrossRef](#)]
30. Millard, M.; Pathania, D.; Grande, F.; Xu, S.; Neamati, N. Small-molecule inhibitors of p53-MDM2 interaction: The 2006–2010 update. *Curr. Pharm. Des.* **2011**, *17*, 536–559. [[CrossRef](#)]
31. Vassilev, L.T. MDM2 inhibitors for cancer therapy. *Trends Mol. Med.* **2007**, *13*, 23–31. [[CrossRef](#)]
32. Zhang, Z.; Chu, X.J.; Liu, J.J.; Ding, Q.; Zhang, J.; Bartkovitz, D.; Jiang, N.; Karnachi, P.; So, S.S.; Tovar, C.; et al. Discovery of potent and orally active p53-MDM2 inhibitors RO5353 and RO2468 for potential clinical development. *ACS Med. Chem. Lett.* **2014**, *5*, 124–127. [[CrossRef](#)]
33. Cui, C.B.; Kakeya, H.; Osada, H. Spirotryprostatin B, a novel mammalian cell cycle inhibitor produced by *Aspergillus fumigatus*. *J. Antibiot.* **1996**, *49*, 832–835. [[CrossRef](#)]
34. Gollner, A.; Rudolph, D.; Arnhof, H.; Bauer, M.; Blake, S.M.; Boehmelt, G.; Cockroft, X.L.; Dahmann, G.; Etmayer, P.; Gerstberger, T.; et al. Discovery of novel spiro [3 H-indole-3, 2'-pyrrolidin]-2 (1 H)-one compounds as chemically stable and orally active inhibitors of the MDM2–p53 interaction. *J. Med. Chem.* **2016**, *59*, 10147–10162. [[CrossRef](#)]
35. Islam, M.S.; Al-Majid, A.M.; El-Senduny, F.F.; Badria, F.A.; Rahman, A.F.M.; Barakat, A.; Elshaier, Y.A. Synthesis, Anticancer Activity, and Molecular Modeling of New Halogenated Spiro [pyrrolidine-thiazolo-oxindoles] Derivatives. *Appl. Sci.* **2020**, *10*, 2170. [[CrossRef](#)]
36. Barakat, A.; Islam, M.S.; Ghawas, H.M.; Al-Majid, A.M.; El-Senduny, F.F.; Badria, F.A.; Elshaier, Y.A.; Ghabbour, H.A. Design and synthesis of new substituted spirooxindoles as potential inhibitors of the MDM2–p53 interaction. *Bioorg. Chem.* **2019**, *86*, 598–608. [[CrossRef](#)]
37. Islam, M.S.; Ghawas, H.M.; El-Senduny, F.F.; Al-Majid, A.M.; Elshaier, Y.A.; Badria, F.A.; Barakat, A. Synthesis of new thiazolo-pyrrolidine–(spirooxindole) tethered to 3-acylindole as anticancer agents. *Bioorg. Chem.* **2019**, *82*, 423–430. [[CrossRef](#)]
38. Lotfy, G.; Aziz, Y.M.A.; Said, M.M.; El Sayed, H.; El Sayed, H.; Abu-Serie, M.M.; Teleb, M.; Dömling, A.; Barakat, A. Molecular hybridization design and synthesis of novel spirooxindole-based MDM2 inhibitors endowed with BCL2 signaling attenuation; a step towards the next generation p53 activators. *Bioorg. Chem.* **2021**, *117*, 105427. [[CrossRef](#)]
39. Aziz, Y.M.A.; Lotfy, G.; Said, M.M.; El Ashry, E.S.H.; El Tamany, E.S.H.; Soliman, S.; Abu-Serie, M.M.; Teleb, M.; Yousuf, S.; Dömling, A. Design, synthesis, chemical and biochemical insights on to novel hybrid spirooxindoles-based p53-MDM2 inhibitors with potential Bcl2 signaling attenuation. *Front. Chem.* **2021**, *9*, 915. [[CrossRef](#)]
40. Popowicz, G.M.; Dömling, A.; Holak, T.A. The structure-based design of MDM2/MDMX–p53 inhibitors gets serious. *Angew. Chem. Int. Ed.* **2011**, *50*, 2680–2688. [[CrossRef](#)]
41. Mrkvová, Z.; Uldrijan, S.; Pombinho, A.; Bartůněk, P.; Slaninová, I. Benzimidazoles downregulate Mdm2 and MdmX and activate p53 in MdmX overexpressing tumor cells. *Molecules* **2019**, *24*, 2152. [[CrossRef](#)]
42. Wu, L.T.; Jiang, Z.; Shen, J.J.; Yi, H.; Zhan, Y.C.; Sha, M.Q.; Wang, Z.; Xue, S.T.; Li, Z.R. Design, synthesis and biological evaluation of novel benzimidazole-2-substituted phenyl or pyridine propyl ketene derivatives as antitumour agents. *Eur. J. Med. Chem.* **2016**, *114*, 328–336. [[CrossRef](#)]
43. Zaytsev, A.; Dodd, B.; Magnani, M.; Ghiron, C.; Golding, B.T.; Griffin, R.J.; Liu, J.; Lu, X.; Micco, I.; Newell, D.R.; et al. Searching for Dual Inhibitors of the MDM2-p53 and MDMX-p53 Protein–Protein Interaction by a Scaffold-Hopping Approach. *Chem. Biol. Drug. Des.* **2015**, *86*, 180–189. [[CrossRef](#)] [[PubMed](#)]
44. Boggu, P.; Venkateswararao, E.; Manickam, M.; Kim, Y.; Jung, S.H. Exploration of SAR for novel 2-benzylbenzimidazole analogs as inhibitor of transcription factor NF-κB. *Arch. Pharm. Res.* **2017**, *40*, 469–479. [[CrossRef](#)] [[PubMed](#)]
45. Błaszczak-Świątkiewicz, K. Antiproliferative aspect of benzimidazole derivatives' activity and their impact on NF-κB expression. *Molecules* **2019**, *24*, 3902. [[CrossRef](#)] [[PubMed](#)]
46. Boggu, P.; Venkateswararao, E.; Manickam, M.; Kwak, D.; Kim, Y.; Jung, S.H. Exploration of 2-benzylbenzimidazole scaffold as novel inhibitor of NF-κB. *Bioorg. Med. Chem.* **2016**, *24*, 1872–1878. [[CrossRef](#)] [[PubMed](#)]
47. Li, J.; Viallet, J.; Haura, E.B. A small molecule pan-Bcl-2 family inhibitor, GX15-070, induces apoptosis and enhances cisplatin-induced apoptosis in non-small cell lung cancer cells. *Cancer Chemother. Pharmacol.* **2008**, *61*, 525–534. [[CrossRef](#)]



48. Barakat, A.; Alshahrani, S.; Al-Majid, A.M.; Alamy, A.S.; Haukka, M.; Abu-Serie, M.M.; Dömling, A.; Mazyed, E.A.; Badria, F.A.; El-Senduny, F.F. Novel spirooxindole based benzimidazole scaffold: In vitro, nanoformulation and in vivo studies on anticancer and antimetastatic activity of breast adenocarcinoma. *Bioorg. Chem.* **2022**, *129*, 106124. [[CrossRef](#)]
49. Vilar, S.; Cozza, G.; Moro, S. Medicinal chemistry and the molecular operating environment (MOE): Application of QSAR and molecular docking to drug discovery. *Curr. Top. Med. Chem.* **2008**, *8*, 1555–1572. [[CrossRef](#)]
50. Salentin, S.; Schreiber, S.; Haupt, V.J.; Adasme, M.F.; Schroeder, M. PLIP: Fully automated protein–ligand interaction profiler. *Nucleic Acids Res.* **2015**, *43*, W443–W447. [[CrossRef](#)]

**Disclaimer/Publisher’s Note:** The statements, opinions and data contained in all publications are solely those of the individual author(s) and contributor(s) and not of MDPI and/or the editor(s). MDPI and/or the editor(s) disclaim responsibility for any injury to people or property resulting from any ideas, methods, instructions or products referred to in the content.